



Universiteit
Leiden
The Netherlands

The role of glomerular filtration and active tubular secretion in predicting renal clearance of drugs in children using population pharmacokinetic and physiology-based pharmacokinetic modeling approaches: unspinning the yarn

Cristea, S.

Citation

Cristea, S. (2021, June 16). *The role of glomerular filtration and active tubular secretion in predicting renal clearance of drugs in children using population pharmacokinetic and physiology-based pharmacokinetic modeling approaches: unspinning the yarn*. Retrieved from <https://hdl.handle.net/1887/3188573>

Version: Publisher's Version

License: [Licence agreement concerning inclusion of doctoral thesis in the Institutional Repository of the University of Leiden](#)

Downloaded from: <https://hdl.handle.net/1887/3188573>

Note: To cite this publication please use the final published version (if applicable).

Cover Page



Universiteit Leiden



The handle <https://hdl.handle.net/1887/3188573> holds various files of this Leiden University dissertation.

Author: Cristea, S.

Title: The role of glomerular filtration and active tubular secretion in predicting renal clearance of drugs in children using population pharmacokinetic and physiology-based pharmacokinetic modeling approaches: unspinning the yarn

Issue Date: 2021-06-16

Estimation of ontogeny functions for renal transporters using a combined population pharmacokinetic and physiology-based pharmacokinetic approach: application to OAT3

S Cristea, EHJ Krekels, K Allegaert, P De Cock,
P De Paepe, A de Jaeger, CAJ Knibbe

AAPS J 23, 65 (2021)

Epub ahead of print, doi.org/10.1208/s12248-021-00595-9

6.1 Abstract

To date, information on the ontogeny of renal transporters is limited. Here we propose to estimate the *in vivo* ontogeny of transporters using a combined population pharmacokinetic (popPK) and physiology-based pharmacokinetic (PBPK) approach (popPBPK). Clavulanic acid and amoxicillin were used as probes for glomerular filtration and for combined glomerular filtration and active secretion through OAT3, respectively. The predictive value of the estimated OAT3 ontogeny function was assessed by PBPK predictions of renal clearance (CL_R) of other OAT3 substrates: cefazolin and piperacillin.

Individual CL_R post-hoc values, obtained from a published popPK model on the concomitant use of clavulanic acid and amoxicillin in children between 1 month to 15 years, were used as dependent variables in the popPBPK analysis. CL_R was re-parameterized according to PBPK principles, resulting in the estimation of OAT3-mediated intrinsic clearance ($CL_{int,OAT3,in vivo}$) and its ontogeny.

$CL_{int,OAT3,in vivo}$ ontogeny was described by a sigmoidal function, reaching half of adult level around 7 months of age, comparable to findings based on renal transporter-specific protein expression data. PBPK-based CL_R predictions including this ontogeny function were reasonably accurate for piperacillin in a similar age range (2.5 months – 15 years) as well as for cefazolin in neonates as compared to published data (%RMSPE of 21.2% and 22.8%, respectively and %PE within $\pm 50\%$).

Using this novel approach we estimated an *in vivo* ontogeny function for $CL_{int,OAT3,in vivo}$ that yields accurate CL_R predictions for different OAT3 substrates across different ages. This approach deserves further study on ontogeny of other transporters.

6.2 Introduction

Pediatric renal clearance (CL_R) is driven by physiology related changes to kidney size, number of glomeruli and nephron filtration capacity, renal blood flow, expression of drug binding plasma proteins and expression of transporters. Throughout the pediatric age-range, the maturation of glomerular filtration rate (GFR) has been extensively studied by various groups [1–6] however less is known about the development of other processes contributing to CL_R such as active tubular secretion (ATS), which is mediated through transporters in the kidneys.

Recently, the ontogeny of individual renal transporters has been quantified by directly measuring transporter-specific protein expressions in postmortem kidney samples from children of different ages [7]. However, there is limited information about how protein expression relates to *in vivo* transporter activity and whether this relationship remains constant with age. Alternatively, ontogeny of ATS has been quantified *in vivo* as net secretion of drugs with non-selective affinity for transporters. Net secretion aggregates the activity of all active secretion transporters involved in renal excretion and of reabsorption [3,8]. Since ontogeny patterns may differ between transporters, their relative contributions to CL_R will also differ throughout the pediatric age-range, as drugs may have a broad spectrum in transporter affinity and can be transported by one or more transporters at once. Therefore, it would be of relevance to separately quantify the ontogeny of each renal transporter *in vivo*.

Empirically, clinical pharmacokinetic (PK) data (i.e. concentration-time data) are analyzed using population PK (popPK) models. When analyzing pediatric PK data, the inter-individual variability in different parameters is driven by differences in underlying developing physiological processes. These differences are usually captured by a function that describes the relation between the individual deviations in parameter values from typical parameter values and a relatively small set of demographic variables that vary with age, i.e. covariate relation. In pediatric physiology-based PK (PBPK) modelling, quantitative knowledge on developing physiology is included a priori in functions that describe changes

in system-specific parameters. Subsequently, these models describe the interaction between drugs with certain physicochemical properties and this system. The parameters in a PBPK model can be derived from various data sources (e.g. in vitro experiments, clinical studies, etc.). Recently, combined popPK and PBPK (popPBPK) approaches have been proposed to derive physiological measures for PBPK models that cannot be obtained through direct measures, by leveraging concentration-time data [9]. When selecting drugs that are predominantly eliminated by one main pathway, inferences can be made regarding system-specific parameters that are particular for that pathway.

In this study, the ontogeny of *in vivo* renal organic anion transporter 3 (OAT3) activity was characterized with this popPBPK approach. To this end, PK data obtained in children of different ages after the concomitant administration of clavulanic acid and amoxicillin was used. Each drug was assumed a probe for their specific elimination pathway, i.e. clavulanic acid for glomerular filtration (GF) and amoxicillin for a combination of GF and ATS through OAT3 [10,11]. With this methodology the ontogeny function of OAT3 could be estimated. Its predictive value was assessed by including the ontogeny function in a pediatric PBPK model to predict CLR of two other OAT3 substrates including cefazolin and piperacillin.

6.3 Methods

6.3.1 Software

For the present analysis we used NONMEM v7.3 integrated with Pirana v2.9.9 for developing the model and R v3.5 integrated with RStudio for graphics and evaluation.

6.3.2 Quantifying the ontogeny function of OAT3 *in vivo*

Individual post-hoc CL_R values for clavulanic acid and amoxicillin in pediatric patients were obtained from a population PK model of De Cock et al. [12]. In short, a simultaneous popPK analysis was performed for both drugs based on data obtained after the administration of a fixed dose ratio of 1:10 (clavulanic acid : amoxicillin) in 50 intensive care pediatric patients with ages between 1 month and 15 years (median age of 2.6 years)[12]. The PK of clavulanic acid and amoxicillin were described by a two- and a three-compartment model, respectively, with inter-individual variability (IIV) on CL_R and central volume of distribution. The covariate analysis identified current weight as a statistically significant predictor for the IIV on both central volume of distribution and CL_R , whereas vasopressor treatment and cystatin C were found to be statistically significant predictors only for the IIV on CL_R [12].

In a sequential step, CL_R was re-parameterized according to PBPK principles to reflect clearance through glomerular filtration (CL_{GF}) and through active tubular secretion (CL_{ATS}). The PBPK-based model for CL_R assumes a serial arrangement for GF and ATS, in which CL_R of clavulanic acid was described by CL_{GF} only ($CL_{ATS} = 0$), while CL_R of amoxicillin was described by a combination of CL_{GF} and CL_{ATS} .

$$CL_R = CL_{GF} + CL_{ATS} = (GFR \times f_u) + \left(\frac{(Q_R - GFR) \times f_u \times CL_{sec,OAT3}}{Q_R + f_u \times \frac{CL_{sec,OAT3}}{BP}} \right) \quad [1]$$

$$CL_{sec,OAT3} = CL_{int,OAT3,in vivo} \times ont_{OAT3} \times PTCPGK \times KW \quad [2]$$

In equation 1, GFR stands for glomerular filtration rate, f_u for drug fraction unbound, Q_R for renal blood flow, $CL_{sec,OAT3}$ for secretion clearance through OAT3, and BP for blood to plasma ratio. Equation 2 shows how $CL_{sec,OAT3}$ is obtained by multiplying $CL_{int,OAT3,in vivo}$ that stands for OAT3-mediated *in vivo* intrinsic clearance in adults, with ont_{OAT3} that stands for the ontogeny function for OAT3, PTCPGK that stands for proximal tubule cells per gram kidney, and KW that stands for kidney weight in grams.

The adult PBPK-based model for CL_R through a combination of GF and ATS (equations 1 and 2) was extrapolated to the pediatric population. For this, published functions that describe the age-related changes of the system-specific parameters (i.e. GFR [14], renal blood flow [15], and kidney weight [15]) and of the drug-specific parameters impacted by changes in system-specific parameters (i.e. serum

albumin concentrations [4] that influence the fraction unbound [16], and hematocrit levels that influence BP [15]) were inputted, as shown in Table S6.1. Values for f_u [17] and BP_{amox} [18] as reported in adults were used ($f_{u,clav.acid} = 0.75$; $f_{u,amox} = 0.82$; $BP_{amox} = 0.55$). $CL_{int,OAT3,in vivo}$ reflects both the expression and activity of the OAT3 transporter in adults. Assuming PTCPGK to remain constant at adult values, this only leaves $CL_{int,OAT3,in vivo}$ and its ontogeny function (ont_{OAT3}) to be estimated. This was done using the individual CL_R values from the population model as dependent variables and deriving the system-specific PBPK parameters based on the individual patient characteristics for each patient.

Pediatric typical CL_{GF} values were obtained using a published GFR maturation function developed for children with a normal renal function [14]. However, when compared to normal CL_{GF} values, CL_R of both drugs as estimated with the population PK models, were found to be increased in the intensive care children included in the dataset of the current analysis [12]. Hence, the PBPK-based re-parameterization of CL_{GF} included a typical GF correction factor (θ_{corr}) with IIV (η_{GFR}) to account for this difference (equations 3).

$$CL_{R,clavulanic\ acid,i} = GFR \times f_{u,clav.\ acid} \times \theta_{corr} \times e^{\eta_{GFR}} \quad [3]$$

As both amoxicillin and clavulanic acid were administered simultaneously to each child, from the data on clavulanic acid the GF correction factor and IIV on GFR for each patient was estimated. According to equations 4 and 5, the difference between the individual values for CL_R of amoxicillin and CL_R of clavulanic acid were used to estimate CL_{AT3} , which was the basis for the estimation of the IIV on the *in vivo* $CL_{sec,OAT3}$ value and subsequently the OAT3 ontogeny function (ont_{OAT3}).

$$CL_{R,amoxicillin,i} = GFR \times f_{u,amox} \times \theta_{corr} \times e^{\eta_{GFR}} + \frac{(Q_R - GFR) \times f_{u,amox} \times CL_{sec,OAT3,i}}{Q_R + f_{u,amox} \times \frac{CL_{sec,OAT3,i}}{BP_{amox}}} \quad [4]$$

$$CL_{sec,OAT3,i} = \theta_{CLint,OAT3,in vivo} \times e^{\eta_{CLint,OAT3,in vivo}} \times ont_{OAT3} \times PTCPGK \times KW \quad [5]$$

To quantify the ontogeny profile of $CL_{int,OAT3,in vivo}$, different covariates (i.e. postnatal age, postmenstrual age, weight) were explored using sigmoid relationships (equation 6) or a simplification of this equation (i.e. an exponential equation). In equation 6, *hill* is the *hill* coefficient, which quantifies the steepness of the ontogeny slope and TM_{50} quantifies the age at which OAT3 reaches half of the adult value.

$$ont_{OAT3} = \frac{COV^{hill}}{COV^{hill} + TM_{50}^{hill}} \quad [6]$$

The statistical significance of including the ont_{OAT3} function in the equation for $CL_{sec,OAT3,i}$ to obtain CL_R of amoxicillin was assessed according to the likelihood ratio test on the difference in objective function value. Under the assumption of a χ^2 distribution, the objective function value of a model with one more degree of freedom had to be 3.84 points lower, with a corresponding $p < 0.05$ to indicate statistical significance [19]. For graphical goodness-of-fit, a plot was made to check for prediction bias of the individual CL_R values obtained either with the PBPK model or the individual post hoc values from the population PK model that served as the dependent variable in these fits. In addition, ETA (η_{GFR} , $\eta_{CLint,OAT3,in vivo}$) vs. covariate plots (age, weight) are made to check for structural accuracy in PK parameters.

6.3.2 Predictive properties of the OAT3 ontogeny function for new substrates

To assess the predictive performance of the obtained OAT3 maturation function, the PBPK model that includes the estimated ontogeny function for OAT3 (equations 1 and 2) was used for pediatric CL_R predictions of piperacillin and cefazolin, two other substrates of the OAT3 transporter. PBPK predictions of CL_R were compared to published pediatric CL_R values of the same drugs. To obtain the pediatric PBPK predictions for CL_R , we collected literature values for f_u , adult of 0.8 (20) and 0.31 (18) for piperacillin and cefazolin, respectively and for BP adult of 0.55 for both drugs. $CL_{int,OAT3,in vivo}$ in equation 2 had to be derived first for both drugs. This was done based on published *in vitro* activity data as measured in assays with OAT3 transfected cells (1.95 μ l/min/mg protein [20] and 7.1 μ l/min/mg protein [18] for piperacillin and cefazolin respectively). These values were used as input for *in vitro-in vivo* extrapolation

(IVIVE). More details on IVIVE are provided in the supplemental materials.

The drug-specific $CL_{int,OAT3, in vivo}$ values obtained in the IVIVE step were used in equations 1 and 2 of the renal PBPK model to obtain pediatric CL_R predictions for cefazolin and piperacillin. Pediatric CL_R predictions for piperacillin and cefazolin were made for typical individuals with the same demographic characteristics as the individual patients reported in the original publications describing the pediatric population PK models of these drugs [12],[21]. This means that, for piperacillin, typical CL_R values were estimated for 47 pediatric patients with ages between 2.5 months and 15 years (median age of 2.83 years). For cefazolin, the typical CL_R values were estimated for 26 near-term neonates with gestational age higher than 35 weeks and postnatal age (PNA) between 1 – 30 days (median of 8 days). For this, the OAT3 ontogeny function obtained above for children of 1 month and older based on data from clavulanic acid and amoxicillin was extrapolated to the neonatal population.

Pediatric PBPK CL_R predictions were visually and quantitatively compared to typical estimates obtained with published population PK models for these two OAT3 substrates. Precision was quantified as percentage root mean square prediction error (%RMSPE) (equation 7) and bias as percentage prediction error (%PE) (equation 8).

$$\%RMSPE = \sqrt{\frac{1}{N} \times \sum_{i=1}^N \left(\frac{CL_{R,PBPK} - CL_{R,reference}}{CL_{R,reference}} \right)^2} \times 100 \quad [7]$$

$$\%PE = \left(\frac{CL_{R,PBPK} - CL_{R,reference}}{CL_{R,reference}} \right) \times 100 \quad [8]$$

In both equations, $CL_{R,PBPK}$ are the CL_R predictions obtained with the renal PBPK model in pediatrics and $CL_{R,reference}$ represents the CL_R values for typical CL_R predictions obtained with the published population PK models [21,22]. %RMSPE and %PE were calculated separately for piperacillin and cefazolin and reported overall as well as per age group. $CL_R,PBPK$ was considered to be accurately predicted if %RMSPE and %PE was within $\pm 30\%$, reasonably accurately predicted between -30% – -50% and 30% – 50% and inaccurate when %RMSPE and %PE were outside $\pm 50\%$. Note that %RMSPE can only take positive values.

6.4 Results

6.4.1 Quantifying the ontogeny function of OAT3

With the popPBPK approach, CL_{GF} was separated from CL_{ATS} such that $CL_{int,OAT3, in vivo}$ and its ontogeny profile could be estimated in children as young as 1-month up to 15 years of age. Figure 6.1 shows the ontogeny profile of OAT3 as best described by a sigmoidal relationship based on PNA. $CL_{int,OAT3, in vivo}$ was estimated to be 15.8 ml/h/g kidney (RSE% of 5%) at 15 years with an IIV of 78.5%. This high IIV suggests large differences between individual values obtained for $CL_{int,OAT3, in vivo}$. $CL_{int,OAT3, in vivo}$ was found to reach half of the adult capacity at a PNA of 27.3 weeks (RSE of 28%), which is around 7 months. The rapid ontogeny of OAT3 was captured by a *hill* exponent of 1.17 (%RSE of 36%). The estimated transporter ontogeny fractions range from 0.1 at 1 month and 1 at 15 years. The GF correction factor used to account for the increased CL_R in intensive care children was estimated at 1.83 (RSE of 4%) with an IIV of 24.4%.

The goodness-of-fit plots did not show any bias for CL_R predictions obtained with CL_R re-parameterized according to PBPK principles. Neither Figure S6.1, which depicts popPBPK CL_R predictions vs. the popPK CL_R predictions, nor Figure S6.2, which depicts the η_{GF} and $\eta_{CL_{int,OAT3, in vivo}}$ vs. covariates (i.e. weight and age) show any bias. This suggests that the PBPK-based re-parameterization as CL_{GF} (equation 3) can predict individual clavulanic acid CL_R values accurately and that the reparameterization for CL_{GF} together with CL_{ATS} (equation 4) can accurately predict the CL_R of amoxicillin as excreted by GF and ATS through OAT3.

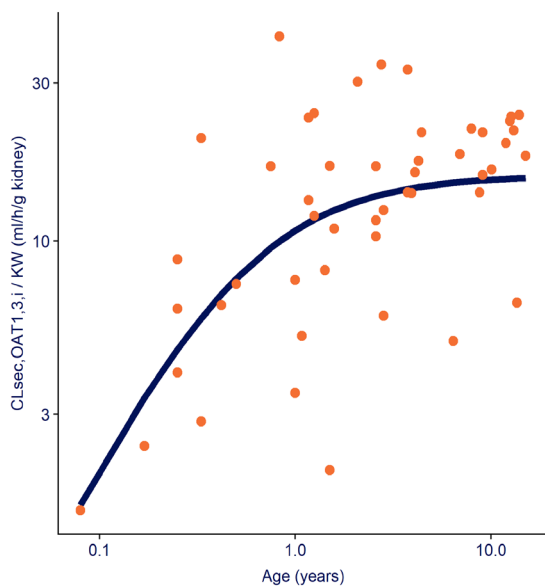


Figure 6.1 Ontogeny function for OAT3-mediated intrinsic clearance normalized by kidney weight ($CL_{sec,OAT3}$ – blue line) described by a sigmoidal function based on age and displayed throughout the studied pediatric age-range (1 month to 15 years), on a double-log scale. The orange dots represent the individual secretion clearance estimates normalized by kidney weight. See equation [5] for more details.

Figure 6.2 shows the total CL_R for amoxicillin and the contribution of CL_{GF} and CL_{ATS} to CL_R for each individual. Total CL_R increases almost 7-fold between neonates younger than 1 year and children of 10 years and older (median of 1.64 L/h and 12 L/h respectively). The median contribution of ATS to amoxicillin CL_R for the studied pediatric population was 22% (range: 4%–40%). Even if variability in ATS contribution was high within groups of individuals with similar ages, the ATS contribution increased with age, on average, from 14% in children younger than 1 year to 18% in children of 1–2 years, 21% for children of 2–5 years, 24% for children 5–10 years, reaching 29% for children older than 10 years.

6.4.2 Predictive properties of the OAT3 ontogeny function for new substrates

Figure 6.2 shows the pediatric CL_R predictions for piperacillin and cefazolin obtained with the PBPK-based model and the identified OAT3 ontogeny function based on clavulanic acid and amoxicillin overlaid with the typical clearance estimates obtained

with the published population PK models. The %RMSPE calculated between PBPK CL_R and typical CL_R predictions for piperacillin (Figure 6.3A) over the entire age-range (2.5 months to 15 years) was 21.8% with a %PE interval between –33.2%–25.4%. When stratified per age groups (i.e. younger than 1 year, 1–2 years, 2–5 years, 5–10 years and older than 10 years) %RMSPE is generally higher for children under 5 years (23.3%, 22.2%, and 27.4% vs. 14.9%, 18.8%). For neonates (Figure 6.3B), the %RMSPE calculated between PBPK CL_R and typical CL_R predictions for cefazolin was 22.2% with %PE interval between –34.4%–46%.

For both pediatric populations the PBPK-based CL_R predictions can be considered reasonably accurate

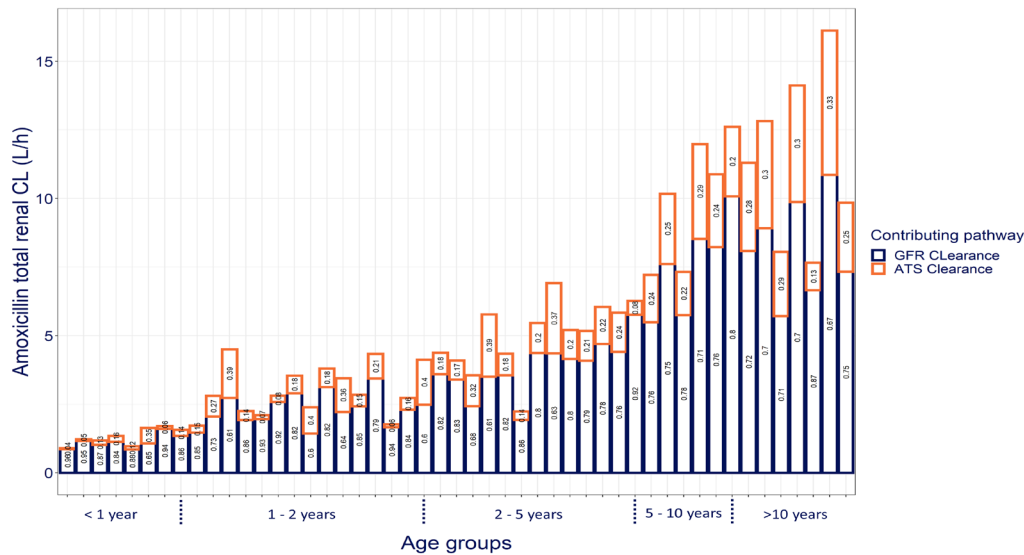


Figure 6.2 Contribution of clearance through glomerular filtration (CL_{GF} – bottom blue boxes) and through active tubular secretion (CL_{ATS} – top orange boxes) to total renal clearance of amoxicillin (CL_R – sum of blue and orange boxes) for each pediatric patient of the studied population sorted and grouped by age. The numbers in each box show the relative contribution of CL_{GF} and CL_{ATS} to total CL_R for each individual

with %RMPE < 30% and %PE within $\pm 50\%$. For piperacillin, the PBPK-based CL_R predictions tend towards overprediction (Figure 6.3A), with all %PE values below 0% although percentages deviation were acceptable [%PE between -13.3% and -28.8%] for children older than 1 year. For cefazolin in neonates, predictions are reasonably accurate (Figure 6.3B), with PBPK-based CL_R predictions tending towards underprediction [%PE between 18.1% and 46%] for children older than 10 days.

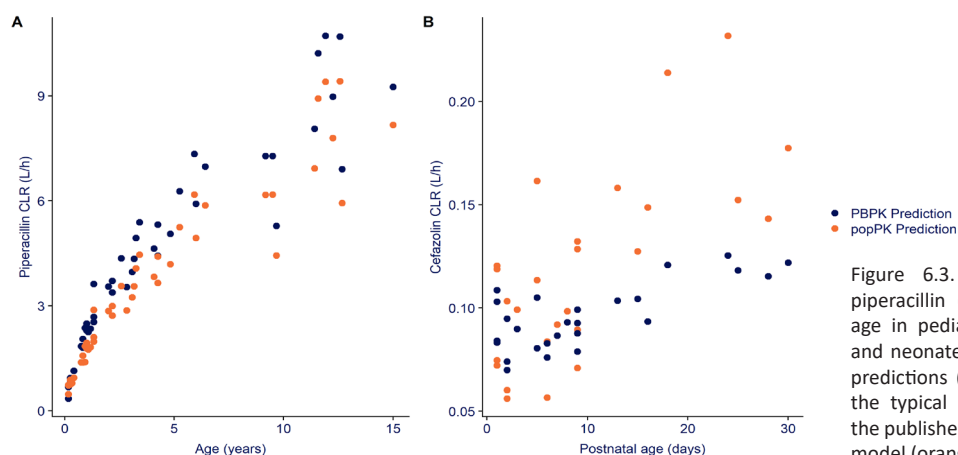


Figure 6.3. Renal clearance (CL_R) of piperacillin (A) and cefazolin (B) versus age in pediatric patients in children (A) and neonates (B). The pediatric PBPK CL_R predictions (dark blue) are overlaid with the typical CL_R estimates obtained with the published population pharmacokinetic model (orange).

6.5 Discussion

With a combined population PK with PBPK approach we estimated the *in vivo* ontogeny function for OAT3, a parameter that cannot be obtained through direct measurements, down to the age of 1 month. With the clinical data available for both clavulanic acid – a descriptor for GF- and amoxicillin – a descriptor for GF and ATS through OAT3- after administration to the same patients simultaneously, we were able to separate the ontogeny in both of these processes. Using a population PK approach, we derived the individual CL_R values for both drugs that served as dependent variable for the popPBPK approach. CL_R was re-parameterized according to PBPK principles to take advantage of existing information about drug- and system-specific properties while estimating the ontogeny of OAT3 *in vivo* and the variability on GFR and on OAT3-mediated intrinsic clearance *in vivo* ($CL_{int,OAT3, in vivo}$).

OAT3 ontogeny for the OAT3-mediated intrinsic clearance is steep in the first year of life, attaining half of the adult value around 7 months of age. This estimated ontogeny function was included in the pediatric PBPK-based model for CL_R through GF and ATS and predicted the CL_R for other drugs that are substrates for OAT3 reasonably accurate, as compared to popPK CL_R predictions for these drugs. Assuming clearance to be only mediated by GF and ATS, for piperacillin the PBPK CL_R predictions over an age-range of 2.5 months to 15 years lead to a %RMSPE of 21.8% [%PE: -33.2%– 25.4%] with a trend towards over-prediction for children older than 1 year. For cefazolin, extrapolation of CL_R predictions to near term neonates with ages between 1- and 30-days lead to a %RMSPE of 22.2% [%PE: -34.4%– 46%], with a trend towards under-prediction for children older than 10 days.

Recently, ontogeny profiles of renal transporters have been quantified based on direct measurements of the expression of transporter-specific proteins in kidney samples taken postmortem from children of various ages, as described in detail by Cheung *et al.* [7]. This group characterized the ontogeny of OAT3 as a sigmoidal function based on PNA in weeks with children reaching half of the adults values around 8 months of age (TM50 = 30.7 weeks [95% CI: 16.64 – 50.97]) and the steepness of the ontogeny slope given by a *hill* coefficient of 0.51 (95% CI: 0.35 – 0.71). While our findings align with Cheung *et al.* regarding the age at which half of the adult level is reached, which was estimated to be around 7 months with our function, we found a steeper ontogeny for OAT3, as shown by a 2-fold higher estimated *hill* coefficient. The impact of these differences on the ontogeny profiles is illustrated in Figure 6.4. This figure shows relatively similar OAT3 ontogeny found by both methods at ages above the TM50 values, but for younger ages the function quantified in our work shows lower ontogeny values. Given the

relatively low number of observed values in both analyses at these younger ages, the uncertainty around the ontogeny below 7 months of age is high for both analyses.

The ontogeny function for OAT3 found in our analysis was included in the pediatric PBPK-based model for CL_R through GF and ATS and used to predict pediatric CL_R for two other substrates for OAT3, namely piperacillin and cefazolin. Despite small trends towards over and under-prediction respectively,

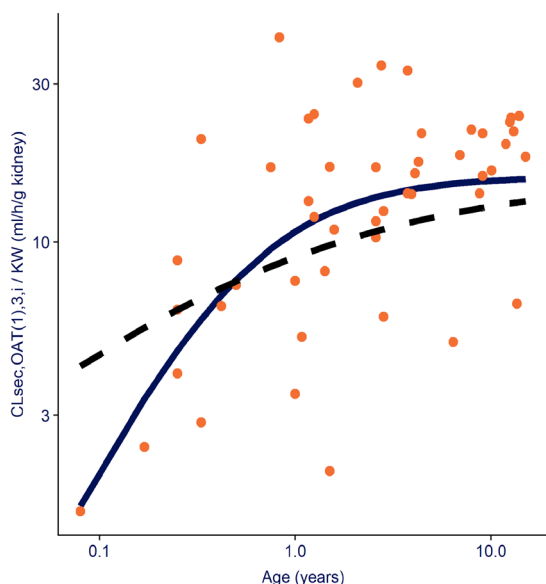


Figure 6.4 Ontogeny functions for OAT3-mediated intrinsic clearance normalized by kidney weight ($CL_{\text{int,OAT3, in vivo}}$) throughout the studied pediatric age-range (1 month to 15 years). The solid line shows the sigmoidal function estimated in the current analysis whereas the dashed line shows the function as published by Cheung *et al.* [7]. The orange dots represent the individual secretion clearance estimates normalized by kidney weight derived from amoxicillin CL_R values obtained with the current analysis. See equation [5] for more details.

CL_R predictions for piperacillin and cefazolin were reasonably accurate with %RMSPE of 21.8% and 22.2%, which is well below the 2-fold error, which is the generally accepted criterion for accuracy of PBPK predictions. The tendency towards over-prediction of pediatric PBPK CL_R for piperacillin could be explained by other processes involved in renal elimination that are not accounted for in the PBPK model. It could, for instance, be that there is passive or active reuptake of these drugs in the kidneys. Alternatively, the authors of the popPK model that served as the reference values, reported a (temporary) impairment of the renal maturation function [22] which could explain the lower CL_R values obtained with the popPK model as compared to the PBPK CL_R predictions, the latter of which does not take (potential) renal impairment into account. A second drug, cefazolin, was used to assess the accuracy of this function for extrapolations to term newborns below 1 month of age. Remarkably, despite a small trend towards under-prediction of CL_R values for cefazolin in part of the newborns, all predictions can still be considered accurate.

Our group recently developed a PBPK simulation framework for investigating the impact of ontogeny of renal secretion transporters on CL_R by predicting pediatric CL_R for hypothetical drugs with an array of drug properties [23]. By looking at the difference between PBPK CL_R predictions with or without inclusion of the ontogeny function, probe drugs for quantifying the ontogeny of transporters were identified. According to the findings with this framework, amoxicillin, which has an estimated $CL_{\text{int,OAT3, in vivo}}$ of 4.4 $\mu\text{l}/\text{min}/\text{mg}$ protein and a f_u of 0.82 [24], has the potential of serving as a probe to quantify OAT3 ontogeny. Furthermore, the clinical data available for probe drugs for GF and a combination of GF and ATS (clavulanic acid and amoxicillin, respectively) administrated to the same individuals was paramount to separate between these two processes.

6.6 Conclusion

The ontogeny of *in vivo* OAT3 activity was quantified by using a combined population PK and PBPK approach. This popPBPK approach leverages the knowledge on underlying physiological processes included in PBPK models and information carried by individual PK parameters as quantified with a population approach, to derive parameters that cannot be measured *in vivo*. With this methodology we derived the renal OAT3 transporter ontogeny *in vivo*. This ontogeny function was included in the pediatric PBPK-based model CL_R for two other OAT3 substrates and on average predicted CL_R throughout the entire pediatric age-range accurately. This methodology could be applied to other transporters substrates to characterize the *in vivo* ontogeny of the remaining renal transporters to further increase our understanding on renal development and increase the accuracy in predicting pediatric CL_R .

6.7 Acknowledgements

The authors would like to thank Dr. Parth Upadhyay for reviewing the code that was used for the analysis presented in this manuscript.

6.8 References

1. Rhodin MM, Anderson BJ, Peters a. M, Coulthard MG, Wilkins B, Cole M, Chatelut E, Grubb A, Veal GJ, Keir MJ, Holford NHG (2009) Human renal function maturation: A quantitative description using weight and postmenstrual age. *Pediatr Nephrol* 24:67–76 . <https://doi.org/10.1007/s00467-008-0997-5>
2. Salem F, Johnson TN, Abduljalil K, Tucker GT, Rostami-Hodjegan A (2014) A re-evaluation and validation of ontogeny functions for cytochrome P450 1A2 and 3A4 based on in vivo data. *Clin Pharmacokinet*. <https://doi.org/10.1007/s40262-014-0140-7>
3. Hayton WL (2000) Maturation and growth of renal function: dosing renally cleared drugs in children. *AAPS PharmSci* 2:E3 . <https://doi.org/10.1208/ps020103>
4. Johnson TN, Rostami-Hodjegan A, Tucker GT (2006) Prediction of the clearance of eleven drugs and associated variability in neonates, infants and children. *Clin Pharmacokinet* 45:931–956 . <https://doi.org/10.2165/00003088-200645090-00005>
5. Mahmood I (2014) Dosing in children: A critical review of the pharmacokinetic allometric scaling and modelling approaches in paediatric drug development and clinical settings. *Clin Pharmacokinet* 53:327–346 . <https://doi.org/10.1007/s40262-014-0134-5>
6. De Cock RFW, Allegaert K, Brussee JM, Sherwin CMT, Mulla H, De Hoog M, Van Den Anker JN, Danhof M, Knibbe C a J (2014) Simultaneous pharmacokinetic modeling of gentamicin, tobramycin and vancomycin clearance from neonates to adults: Towards a semi-physiological function for maturation in glomerular filtration. *Pharm Res* 31:2643–2654 . <https://doi.org/10.1007/s11095-014-1361-z>
7. Cheung KWK, van Groen BD, Spaans E, van Borselen MD, de Bruijn ACJM, Simons-Oosterhuis Y, Tibboel D, Samsom JN, Verdijk RM, Smeets B, Zhang L, Huang SM, Giacomini KM, de Wildt SN (2019) A Comprehensive Analysis of Ontogeny of Renal Drug Transporters: mRNA Analyses, Quantitative Proteomics, and Localization. *Clin Pharmacol Ther*. <https://doi.org/10.1002/cpt.1516>
8. Rubin MI, Bruck E, Rapoport M, Snively M, McKay H, Baumler a (1949) Maturation of Renal Function in Childhood: Clearance Studies. *J Clin Invest* 28:1144–62 . <https://doi.org/10.1172/JCI102149>
9. Tsamandouras N, Rostami-Hodjegan A, Aarons L (2015) Combining the “bottom up” and “top down” approaches in pharmacokinetic modelling: Fitting PBPK models to observed clinical data. *Br J Clin Pharmacol*. <https://doi.org/10.1111/bcp.12234>
10. Parvez MM, Kaiser N, Shin HJ, Jae Lee Y, Shin J-G (2018) Comprehensive Substrate Characterization of 22 Antituberculosis Drugs for Multiple Solute Carrier (SLC) Uptake Transporters In Vitro. *Antimicrob Agents Chemother* 62:1–12
11. Horber FF, Frey FJ, Descoedres C, Murray AT, Reubi FC (1986) Differential effect of impaired renal function on the kinetics of clavulanic acid and amoxicillin. *Antimicrob Agents Chemother*. <https://doi.org/10.1128/AAC.29.4.614>
12. De Cock PAJG, Standing JF, Barker CIS, De Jaeger A, Dhont E, Carlier M, Verstraete AG, Delanghe JR, Robays H, De Paepe P (2015) Augmented Renal Clearance Implies a Need for Increased Amoxicillin-Clavulanic Acid Dosing in Critically Ill Children. *Antimicrobial Agents and Chemotherapy* Oct 2015, 59 (11) 7027-7035; DOI: 10.1128/AAC.01368-15
13. Salem F, Johnson TN, Abduljalil K, Tucker GT, Rostami-Hodjegan A (2014) A re-evaluation and validation of ontogeny functions for cytochrome P450 1A2 and 3A4 based on in vivo data. *Clin Pharmacokinet* 53:625–636 . <https://doi.org/10.1007/s40262-014-0140-7>

14. Simcyp (a Certara Company) (2018) Simcyp v18
15. McNamara PJ, Alcorn J (2002) Protein binding predictions in infants. *AAPS PharmSci*. <https://doi.org/10.1208/ps040104>
16. FDA Augumentin ES-600: Prescribing information. https://www.accessdata.fda.gov/drugsatfda_docs/label/2009/050755s014lbl.pdf
17. Mathialagan S, Piotrowski MA, Tess DA, Feng B, Litchfield J, Varma M V. (2017) Quantitative prediction of human renal clearance and drug-drug interactions of organic anion transporter substrates using in vitro transport data: A relative activity factor approach. *Drug Metab Dispos*. <https://doi.org/10.1124/dmd.116.074294>
18. Nguyen THT, Mouksassi MS, Holford N, Al-Huniti N, Freedman I, Hooker AC, John J, Karlsson MO, Mould DR, Perez Ruixo JJ, Plan EL, Savic R, Van Hasselt JGC, Weber B, Zhou C, Comets E, Mentre F (2017) Model evaluation of continuous data pharmacometric models: Metrics and graphics. *CPT Pharmacometrics Syst Pharmacol*. <https://doi.org/10.1002/psp4.12161>
19. Wen S, Wang C, Duan Y, Huo X, Meng Q, Liu Z, Yang S, Zhu Y, Sun H, Ma X, Yang S, Liu K (2018) OAT1 and OAT3 also mediate the drug-drug interaction between piperacillin and tazobactam. *Int J Pharm*. <https://doi.org/10.1016/j.ijpharm.2017.12.037>
20. De Cock RFW, Smits a., Allegaert K, de Hoon J, Saegeman V, Danhof M, Knibbe C a J (2014) Population pharmacokinetic modelling of total and unbound cefazolin plasma concentrations as a guide for dosing in preterm and term neonates. *J Antimicrob Chemother* 69:1330–1338 . <https://doi.org/10.1093/jac/dkt527>
21. De Cock PAJG, van Dijkman SC, de Jaeger A, Willems J, Carlier M, Verstraete AG, Delanghe JR, Robays H, Walle J Vande, Della Pasqua OE, De Paepe PD (2017) Dose optimization of piperacillin/tazobactam in critically ill children. *J Antimicrob Chemother* 72:2002–2011 . <https://doi.org/10.1093/jac/dkx093>
22. Cristea S, Calvier EAM, Rostami-Hodjegan A, Krekels EHJ, Knibbe CAJ (2015) Impact of renal transporters on pediatric renal clearance using PBPK modelling Discover the World at Leiden University. 2015
23. FDA (2008) AUGMENTIN® (amoxicillin/clavulanate potassium) Powder for Oral Suspension and Chewable Tablets. https://www.accessdata.fda.gov/drugsatfda_docs/label/2008/050575s037550597s044050725s025050726s019lbl.pdf
24. T'jollyn H, Snoeys J, Van Bocxlaer J, De Bock L, Annaert P, Van Peer A, Allegaert K, Mannens G, Vermeulen A, Boussery K (2017) Strategies for Determining Correct Cytochrome P450 Contributions in Hepatic Clearance Predictions: In Vitro–In Vivo Extrapolation as Modelling Approach and Tramadol as Proof-of Concept Compound. *Eur J Drug Metab Pharmacokinet*. <https://doi.org/10.1007/s13318-016-0355-0>
25. Brill MJE, Houwink API, Schmidt S, Van dongen EP a, Hazebroek EJ, Van ramshorst B, Deneer VH, Mouton JW, Knibbe C a J (2014) Reduced subcutaneous tissue distribution of cefazolin in morbidly obese versus non-obese patients determined using clinical microdialysis. *J Antimicrob Chemother* 69:715–723 . <https://doi.org/10.1093/jac/dkt444>
26. Butterfield JM, Lodise TP, Beegle S, Rosen J, Farkas J, Pai MP (2014) Pharmacokinetics and pharmacodynamics of extended-infusion piperacillin/tazobactam in adult patients with cystic fibrosis-related acute pulmonary exacerbations. *J Antimicrob Chemother*. <https://doi.org/10.1093/jac/dkt300>

6.9 Supplementary material

Table S6.1 Functions describing age-related changes of system-specific parameters and variables required by the PBPK model for pediatric CL_R predictions

System-specific parameters for equation [1] (abbreviation) [units]	Maturation functions included in the pediatric PBPK model for CL _R
Glomerular filtration rate (GFR) [ml/min]	$GFR = 112 \times \left(\frac{WT}{70}\right)^{0.63} \times \left(\frac{PMA^{3.3}}{PMA^{3.3} + 55.4^{3.3}}\right)$
Fraction unbound (fu) [-]	$[HSA]_{ped/adult} = 1.1287 \times \ln(AGE) + 33.746$ $f_{u,clav.acid} = 0.75; f_{u,amox.} = 0.82 \text{ (adult values)}$ $\rightarrow f_{u,ped} = \frac{1}{1 + \frac{(1-f_{u,drug}) \times [HSA]_{ped}}{[HSA]_{adult} \times f_{u,drug}}}$
Renal blood flow (QR) [ml/min]	$CO = BSA \times (110 + 184 \times e^{-0.0378 \times AGE} - e^{-0.24477 \times AGE})$ $fr = \frac{fr_{males} + fr_{females}}{2}$ $fr_{males} = 4.53 + \left(14.63 \times \frac{AGE}{0.1888 + AGE}\right)$ $fr_{females} = 4.53 + \left(13 \times \frac{AGE^{1.15}}{0.188^{1.15} + AGE^{1.15}}\right)$ $\rightarrow QR = CO \times fr$
Intrinsic secretion CL (CL _{sec,OAT3}) [mL/min]	$PTCPKG = 60 \text{ (adult value)}$ $KW = 1050 \times (4.214 \times WT^{0.823} + 4.456 \times WT^{0.795}) / 1000$ $\rightarrow CL_{sec,OAT3} = CL_{int,OAT3,in vivo} \times ont_{OAT3} \times PTCPKG \times KW$
Blood to plasma ratio (BP _{amoxicillin}) [-]	$hemat = \frac{hemat_{male} + hemat_{female}}{2}$ $hemat_{male} = 53 - \left(\left(43 \times \frac{AGE^{1.12}}{0.05^{1.12} + AGE^{1.12}} \right) \times \left(1 + \left(-0.93 \times \frac{AGE^{0.25}}{0.10^{0.25} + AGE^{0.25}} \right) \right) \right)$ $hemat_{female} = 53 - \left(\left(37.4 \times \frac{AGE^{1.12}}{0.05^{1.12} + AGE^{1.12}} \right) \times \left(1 + \left(-0.80 \times \frac{AGE^{0.25}}{0.10^{0.25} + AGE^{0.25}} \right) \right) \right)$ $\rightarrow BP = 1 + hemat \times (f_u \times k_p - 1)$

WT – bodyweight [kg]

PMA – postmenstrual age [weeks]

[HSA] – human serum albumin [g/L]

CO – cardiac output [mL/min]

hemat – hematocrit

fr – fraction of cardiac output directed to renal artery

AGE – age in [days] for the maturation of [HSA] and in [years] for the fraction of cardiac output and hematocrit levels

BSA – body surface area (m²)

PTCPKG – proximal tubule cells per gram kidney [x 106 cells]

KW – kidney weight [g]

ont_{OAT3} – OAT3 ontogeny relative to adult levels [-]

CL_{int,OAT3} – OAT3-mediated active clearance [mL/min]

k_p – blood-to-plasma partitioning coefficient of a drug

S6.8.1 In vitro – in vivo extrapolation (IVIVE)

The CL_{int,OAT3,in vivo} values required for the PBPK-based model for CL_R (equation 1 and 2 of the main document), were obtained following *in vitro-in vivo* extrapolation, as shown in equation S1. Published *in vitro* values for OAT3-mediated intrinsic clearance (CL_{int,OAT3,in vitro}) for piperacillin and cefazolin [20],[18] obtained from tissue samples from adults (Table 6.8.1.1), were extrapolated to CL_{int,OAT3,in vivo} based on the protein expression correction factor (relative active factor (RAF)) between the OAT-transfected cells in the *in vitro* assay and the in proximal tubule cells and an activity adjustment factor (AAF).

$$CL_{int,OAT3,in vivo} = CL_{int,OAT3,in vitro} \times \text{protein correction} \times \text{RAF} \times \text{AAF}, \quad [S1]$$

In equation S1, protein correction represents the total amount of proteins in 106 cells obtained from the *in vitro* sample, under the assumption that 106 cells from this sample is equivalent to 106 proximal tubule cells in the kidney. RAF is an activity correction factor between the *in vitro* and the *in vivo* OAT3 transporter activity. These first two parameters are specific to the *in vitro* assay and independent of the

studied drug. AAF is the activity adjustment factor, which is included as a correction factor for $CL_{int,OAT3,in vitro}$ to account for the discrepancy between the CL_R obtained with adult PBPK model and the reported CL_R values in literature [25].

For performing IVIVE, a protein expression value of 0.25 mg protein per 106 Human Embryonic Kidney 293 (HEK293) OAT-transfected cells was used as measured and reported by Mathialagan [18] for their uptake assay [18]. For cefazoline, $CL_{int,OAT3,in vitro}$ was measured by the same group, whereas for piperacillin this value was obtained from a similar system but developed by another research group (Wen et al. [20]). Since the protein expression value is not reported for Wen et al. [20], the protein expression value was assumed to be the same between cell systems and included as such for the IVIVE.

The RAF value used for OAT3 was previously determined by Mathialagan [18] by using selective substrates for OAT transporters to account for the difference between the scaled *in vitro* and *in vivo* intrinsic secretion clearance ($CL_{sec,OAT}$ – equation 2 of the main document). For OAT3, the reported value was 4.6 and this drug-independent value was included as such in equation S1.

AAF was obtained by back-calculation to match the literature values collected for CL_R . Using the literature adult CL_R , the PBPK model was then solved for $CL_{sec,OAT3}$ as shown in equation S2A. The result was used in equation S3A, which was solved for $CL_{int,OAT3,in vivo}$. The obtained $CL_{int,OAT3,in vivo}$ was used as input in equation S4A, solved for AAF. This factor was then multiplied with the relevant parameter to obtain the *in vivo* OAT3-mediated intrinsic clearance. AAF accounts for any activity differences between *in vitro* assays and *in vivo* derived activity in adults [25].

$$CL_{R,lit.} = f_u \times GFR + \frac{(Q_R - GFR) \times f_u \times CL_{sec,OAT3}}{Q_R + f_u \times \frac{CL_{sec,OAT3}}{BP}} \quad [S2]$$

$$CL_{sec,OAT3} = \frac{(CL_{R,lit.} - f_u \times GFR) \times Q_R}{((Q_R - GFR) \times f_u - (CL_R - f_u \times GFR) \times \frac{f_u}{BP})} \quad [S2A]$$

$$CL_{sec,OAT3} = ont_{OAT3} \times CL_{int,OAT3} \times PTCPGK \times KW \quad [S3]$$

$$CL_{int,OAT3} = \frac{CL_{sec,OAT3}}{ont_{OAT3} \times PTCPGK \times KW} \quad [S3A]$$

$$CL_{int,OAT3,in vivo} = CL_{int,OAT3,in vitro} \times protein\ expression \times RAF \times AAF, \quad [S4]$$

$$AAF = \frac{CL_{int,OAT3,in vivo}}{CL_{int,OAT3,in vitro} \times protein\ expression \times RAF} \quad [S4A]$$

The drug-specific parameters required as input for the PBPK-based model (i.e. f_u and BP) were collected from literature for each drug [26,27] (Table S6.2). Literature values of adult CL_R for cefazolin and piperacillin were collected together with the reported median values of the demographic characteristics in these reports (i.e. weight, age) (Table S6.2), as these values were needed to derive the system-specific parameters required in equations S2 and S3 (i.e. GFR, QR, KW, HSA concentration). As the PBPK model is for adults, ont_{OAT3} was fixed at the adult level ($ont_{OAT3} = 1$). The $CL_{int,OAT3,in vivo}$ obtained after the IVIVE step in adults was included in the pediatric PBPK model for CL_R .

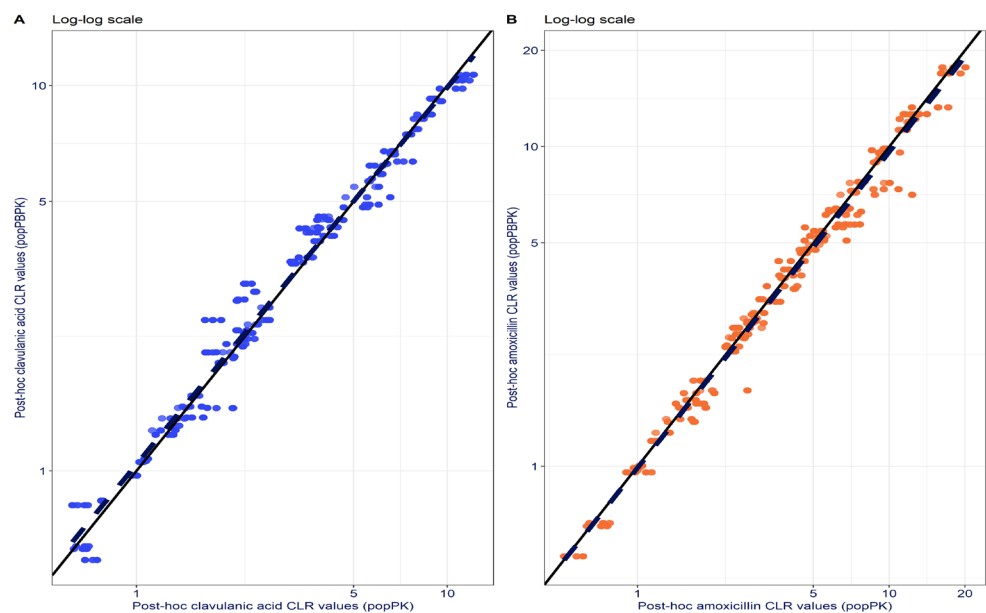


Figure S6.1 Individual post-hoc CL_R predictions of clavulanic acid (left panel) and amoxicillin (right panel) obtained with the population PK approach vs. individual post-hoc CL_R predictions obtained with the combined population and PBPK approach (popPBPK). A line of identity (solid line) and a linear regression line (dashed line) are added to the graph. The data points are scattered around the line of identity without bias. Plots are on a double-log scale.

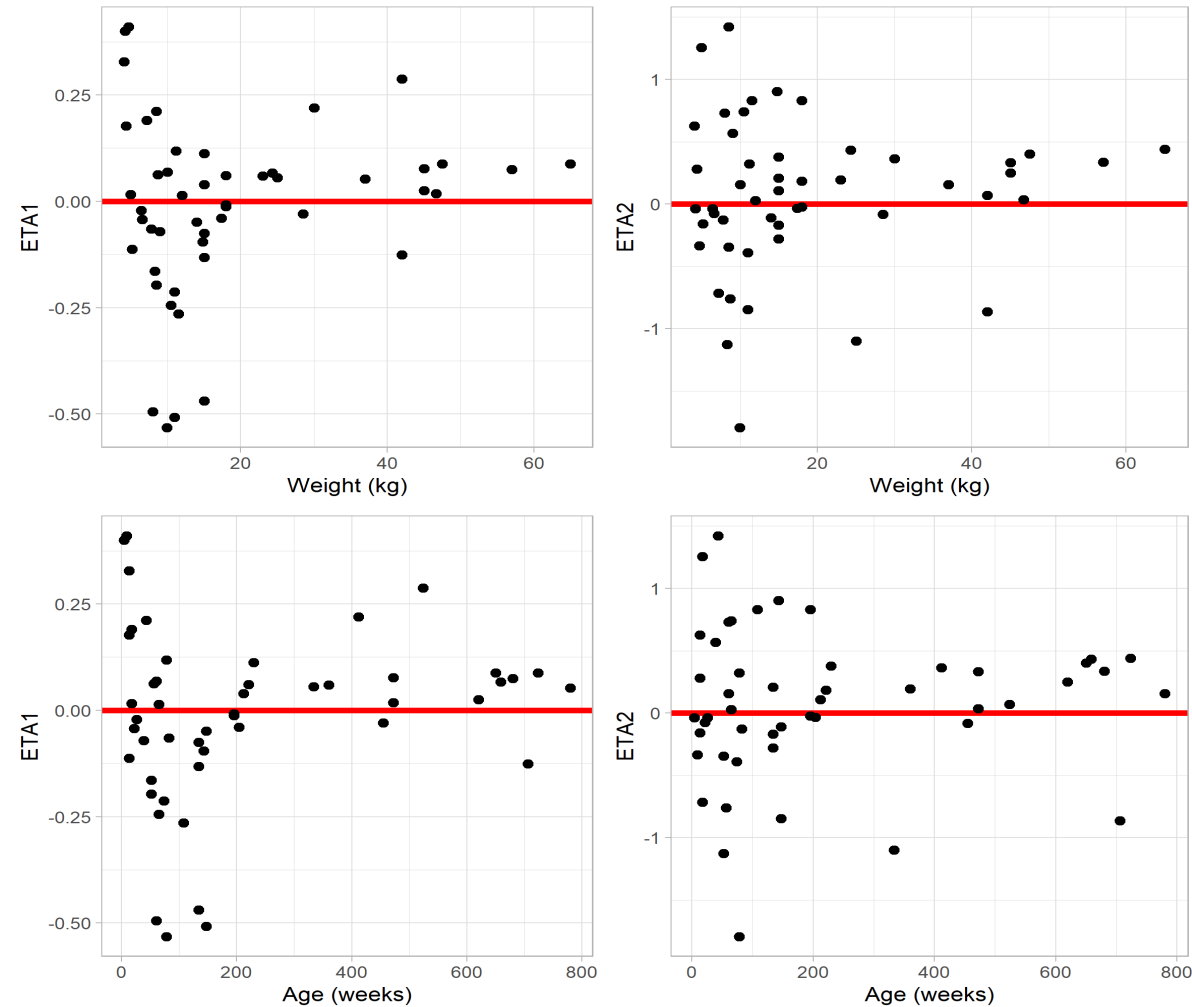


Figure S6.2 ETA vs. covariates correlation plots. This shows the correlation between $\eta_{CL_{int,OAT3,in vivo}}$ (ETA1) and η_{GFR} (ETA2) as estimated with the popPBPK approach and weight and postnatal age in weeks, in the model including the ontogeny function for OAT3. Red line is the zero line, the theoretical mean of the ETAs

Table S6.2 Adult demographic characteristics and drug-specific parameters used for PBPK-based CL_R predictions as well as published typical CL_R values for adults as obtained with popPK models, for piperacillin and cefazolin.

		Piperacillin value [unit]	Cefazolin value [unit]
Demographic characteristics	Weight	53.6 [kg]	109 [kg]
	Age	33 [years]	47 [years]
Drug-specific parameter	$CL_{int,OAT3, \text{ in vitro}}$	1.95 [$\mu\text{l}/\text{min}/\text{mg protein}$][20]	7.1 [$\mu\text{l}/\text{min}/\text{mg protein}$][18]
CL_R values	Total CL_R (literature)	13.6 [L/h](27)	4.5 [L/h](26)
	Activity adjustment factor (AAF)	11.6	0.65

6.10 NONMEM model code

```

$PROBLEM Estimation of transporters ontogeny
$INPUT ID TIME DV MDV CL3i CL4i CL5i V1i V2i V3i V4i V5i DOSN SEX AGE PMA
LENGTH WT BSA PRISM PELOD BLQ CMT COVCYS1i COVCYS2i COVVASi CYSC AMT RATE
INF L2 EVID
$DATA coamox_sinzi_indivparms_4.csv IGNORE=#; input datafile
      IGNORE(ID.EQ.25)
$SUBROUTINE ADVAN13 TOL=9

$MODEL
NCOMP = 5
COMP(CENTRAL)
COMP(PERIPH1)
COMP(PERIPH2)
COMP(CENTRAL)
COMP(PERIPH)

$PK
; include/align units for covariates needed -----

WTG = WT * 1000      ; weight from kg to g
AGED = AGE * 365     ; age in days
HSA_AD = 44          ; g/dl
FU_CLAV = 0.75       ; between 0.7-0.8 for clavulanic acid
FU_AMOX = 0.82       ; determined in vitro
BP2 = 0.55           ; blood-to-plasma partition coefficient for amoxicillin

; fixed PBPK functions -----

; GFR -----
GFR = 112 * ((WTG/70000) ** 0.632) * (PMA ** 3.3) / ((PMA ** 3.3) + (55.4 **
3.3)) * 0.06          ; GFR in L/h
HSA = 1.1287 * LOG(AGED) + 33.764      ; HSA pediatrics
FU1 = 1 / (1 + ((1 - FU_CLAV) * HSA) / (HSA_AD * FU_CLAV)) ; fu clavulanic acid
FU2 = 1 / (1 + ((1 - FU_AMOX) * HSA) / (HSA_AD * FU_AMOX)) ; fu amoxicillin

; active tubular secretion -----
CO = BSA * (110 + 184 * EXP(-0.0378 * AGE) - EXP(-0.24477 * AGE)) ; L/h
IF(SEX.EQ.0) THEN      ; fraction of CO for females
      FRCO = 4.53 + (13.00 * AGE ** 1.15 / (0.188 ** 1.15 + AGE ** 1.15))
ENDIF

IF(SEX.EQ.1) THEN ; fraction of CO for male
      FRCO = 4.53 + (14.63 * AGE ** 1.0 / (0.188 ** 1.0 + AGE ** 1.0))
ENDIF

QR = FRCO * CO ; L/h ; renal blood flow

; density of kidney x kidney volume = kidney weight in grams
KW = 1050 * (4.214 * WT ** 0.823 + 4.456 * WT ** 0.795) / 1000

; covs relationships fixed from PPK model -----
COVCYS1 = COVCYS1i ; (CYSC/0.63) ** THETA(11) ; amoxicillin
COVCYS2 = COVCYS2i ; (CYSC/0.63) ** THETA(12) ; clavulanic acid
COVVAS = COVVASi

; parms to be estimated -----
MAT = THETA(3) + (THETA(4) - THETA(3)) * (AGED/7) ** THETA(5) / (THETA(6) **
THETA(5) + (AGED/7) ** THETA(5)) ; maturation func OAT3

```

```

CLINT = THETA(2)/100 * MAT * KW ; intrinsic CL scaled by 100
ATS = ((QR - GFR) * FU2 * CLINT / (QR + FU2 * CLINT/BP2)) * EXP(ETA(2))
GFRCL = (GFR * THETA(1) * FU2) * EXP(ETA(1))
CL1 = (GFRCL + ATS) * COVCYS1 * COVVAS ; CL amoxicillin
CL2 = (GFR * THETA(1) * FU1) * EXP(ETA(1)) * COVCYS2 ; CL clavulanic acid

; --- posthoc estimates from PPK model
Q11 = CL3i ; intercompartmental CL amox
Q21 = CL4i ; intercompartmental CL clav ac.
Q12 = CL5i ; intercompartmental CL amox (2)
V11 = V1i ; central volume amox.
V21 = V2i ; central volume clav. ac.
V12 = V3i ; peripheral volume amox. (1)
V22 = V4i ; peripheral volume clav. ac.
V13 = V5i ; peripheral volume amox. (2)

K10 = CL1/V11 ; elimination rate amox
K20 = CL2/V21 ; elimination rate for clav. ac.
K13 = Q11/V11 ; intercompartmental rate amox. central -> periph 1
K15 = Q12/V11 ; intercompartmental rate amox. central -> periph 2
K24 = Q21/V21 ; intercompartmental rate clav. ac. central -> periph
K31 = Q11/V12 ; intercompartmental rate amox. periph 1 -> central
K42 = Q21/V22 ; intercompartmental rate clav. ac. periph -> central
K51 = Q12/V13 ; intercompartmental rate amox. periph 2 -> central

S1 = V11 ; scaling amoxi.
S2 = V21 ; scaling clav. ac.

$DES
DADT(1) = A(3) * K31 + A(5) * K51 - A(1) * (K10+K13+K15) ; 1 central amox.
DADT(2) = A(4) * K42 - A(2) * (K20 + K24) ; 2 central clav. ac.
DADT(3) = A(1) * K13 - A(3) * K31 ; 3 periph. cmp. amox.
DADT(4) = A(2) * K24 - A(4) * K42 ; 4 periph. cmp. clav. ac.
DADT(5) = A(1) * K15 - A(5) * K51 ; 5 periph. cmp. (2) amox.

$ERROR
IPRED = F

C1 = A(1) / V11 ; conc. amox.
C2 = A(2) / V21 ; conc. clav.

IND1 = 0
IND2 = 0
IF(CMT.EQ.1) IND1 = 1
IF(CMT.EQ.2) IND2 = 1
Y1 = C1 * (1 + ERR(1))
Y2 = C2 * (1 + ERR(2))
Y = Y1*IND1 + Y2*IND2

; Initial estimates (lower boundary, initial) for typical parameters
$THETA
(0, 2) ; 1- augmented CL amox.
(0, 2) ; 2- CL clav. ac.
0 FIX ; 3- Fbirth
1 FIX ; 4- Adult max
(0, 0.5) ; 5- HILL
(0, 31) ; 6- Age of half maturation

; Initial estimates between-subject variability variance
$OMEGA
0.06 ; IIV CL amox.
0.6 ; IIV CL clav. ac.

```

```

; Residual variability
$SIGMA BLOCK(2)      ;covariance for prop. residual random effects
0.11
0.009 0.12

; Estimation method
$ESTIMATION METHOD=1 INTER MAXEVAL=9999 NOABORT SIG=3 PRINT=1 POSTHOC

; Covariance step
$COVARIANCE PRINT = E

; Output table
$TABLE ID TIME DV IPRED PRED CWRES CWRESI MDV CL1 CL2 Q12 Q21 Q11 V11 V21
V12 V13 V22 ETA1 ETA2 C1 C2 GFR FU1 FU2 HSA CO QR SEX AGE PMA WT BSA PRISM
PELOD COVCYS1 COVCYS2 COVVAS BLQ CYSC MAT CMT RES WRES CLINT ATS GFRCL
NOPRINT NOAPPEND ONEHEADER FILE=run303_6_201.tab

```

